Journal of
Materials Chemistry A

Accepted Manuscript

This article can be cited before page numbers have been issued, to do this please use: C. Cuadrado Collados, J. Fernandez-Catalá, F. Fauth, Y. Cheng, L. L. Daemen, A. J. Ramirez-Cuesta and J. Silvestre-Albero, *J. Mater. Chem. A*, 2017, DOI: 10.1039/C7TA05922A.

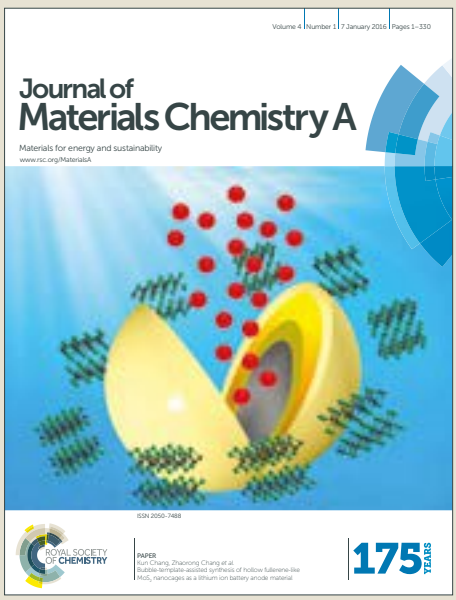

ROYAL SOCIETY OF CHEMISTRY

rsc.li/materials-a

View Article Online
DOI: 10.1039/C7TA05922A

Understanding the breathing phenomena in nano-ZIF-7 upon gas adsorption

Carlos Cuadrado-Collados,[1] Javier Fernández-Català,[1] François Fauth,[2] Yongqiang Q. Cheng,[3] Luke L. Daemen,[3] Anibal J. Ramirez-Cuesta,[3] Joaquín Silvestre-Albero[1,*]

[1] Laboratorio de Materiales Avanzados, Departamento de Química Inorgánica-Instituto Universitario de Materiales, Universidad de Alicante, Ctra. San Vicente-Alicante s/n, E-03690 San Vicente del Raspeig, Spain
[2] CELLS-ALBA Synchrotron, E-08290 Cerdanyola del Vallés, Barcelona, Spain
[3] Oak Ridge National Laboratory, Chemical and Engineering Materials Division, 1 Bethel Valley Road, Oak Ridge, Tennessee 37831, USA

Abstract

Synchrotron X-ray diffraction and inelastic neutron scattering measurements have been applied to evaluate the breathing phenomena in small nanocrystals of ZIF-7 upon gas adsorption. Experimental results show that an extended solvent exchange process with methanol is crucial to get a solvent-free narrow pore structure. Under these conditions, nano-ZIF-7 is indeed able to adsorb N_2 with a total BET surface area around 380 m^2/g, in close agreement with theoretical predictions. The breathing phenomenon upon nitrogen adsorption is accompanied by a phase-to-phase transition, from narrow-pore (phase II) to a large-pore (phase I) structure and a suppression of the cooperative deformation of the framework involving mainly the flapping motion of the benzimidazolate (bIm) ligand with the 4- and 6-membered rings. Whereas nitrogen requires temperature and pressure conditions close to condensation (close to 1 bar and 77K) to induce the breathing in ZIF-7, CO_2 can do it under milder conditions (room temperature and at extremely low relative pressures). These results reflect that the nature of the probe adsorptive rather than the molecular diameter and/or shape, and the gas-framework interactions play a crucial role defining the pressure and temperature conditions to induce the breathing. The presence of two different cavities in ZIF-7 as suggested by theoretical predictions, one with a window diameter below 0.4 nm (cavity A) and a second one with a pore size around 0.6 nm (cavity B), have been confirmed experimentally using immersion calorimetry.

View Article Online
DOI: 10.1039/C7TA05922A

Introduction

Understanding structural flexibility in nanoporous solids upon an external stimuli (for instance upon a pressure or temperature change, or upon gas exposure) is of paramount importance to define their performance in a subsequent application (e.g., sensors, gas separation units, drug-delivery devices, etc.). Despite the importance of these processes under *operando* conditions, they have been scarcely described in the literature due to the difficulty in their identification, preferentially for amorphous materials (for instance, activated carbons).[1-4] Among nanoporous solids with associated framework dynamics, zeolitic imidazole frameworks (ZIFs) are by far the most widely investigated in the last few years.[5,6] The large interest attracted by these materials is due to their highly developed porous structure, large crystallinity, and high thermal and mechanical stability (the metal–imidazolate-type ligand–metal bond angle resemble that of the Si–O–Si in zeolites).[5-7]

Among zeolitic imidazolate frameworks, ZIF-8 is by far the most widely investigated. ZIF-8, the zinc imidazolate framework, has been traditionally associated with two distinct structural phenomena upon gas adsorption (e.g., N_2). A gate opening phenomena at low pressures (< 0.01 bar) and a slight framework expansion (< 1%) upon an increase in the nitrogen partial pressure to ≈ 0.02-0.03 bar has been clearly identified.[8-10] Recent studies using inelastic neutron scattering (INS) under *operando* conditions have shown that the gate-opening phenomena in ZIF-8 is indeed associated with the swinging of the $–CH_3$ groups from the imidazolate linker upon gas adsorption.[10] Furthermore, these studies have shown that the swinging phenomenon highly depends in the nature of the adsorbed molecule, i.e. N_2 and CO does while Ar and O_2 does not.[11] ZIF-7 is a closely related

View Article Online
DOI: 10.1039/C7TA05922A

material to ZIF-8 sharing the same metal ion (Zn), the only difference being the nature of the ligand, i.e. benzimidazolate ligand ($Zn(bIm)_2$) in the former case. Although both coordination polymers exhibit the same SOD topology with 4- and 6-membered ring windows, their crystal structure is completely different (ZIF-8 exhibit a cubic structure whereas ZIF-7 exhibits trigonal symmetry), as well as their structural performance against a external stimuli (pressure or temperature change). Whereas ZIF-8 exhibits a gate-opening phenomena and a certain structural expansion upon gas exposure, ZIF-7 is associated with a phase–to–phase transition upon gas exposure (only data for CO_2 have been reported so far) or after a thermal treatment.[12-16] This structural transition involves a crystallographic change from a high-density phase II structure, with triclinic symmetry, also called narrow pore (np), to a low-density phase I structure with trigonal symmetry, also called large pore (lp). Despite the importance of this reversible phase transition, the breathing phenomena in ZIF-7 has been scarcely evaluated due to the difficulty to properly remove the solvent and to get an empty pore, fully accessible, ZIF-7 structure. Indeed, traditional synthesis for ZIF-7 involves N,N-dimethylformamide (DMF) as a solvent with the associated difficulty to completely remove DMF from the inner cavities.[13, 17, 18]

With this in mind, the main goal of this manuscript is to evaluate the breathing phenomena in small nanocrystals of ZIF-7 prepared using a solvent exchange approach. Under these conditions we will be able to completely remove unreacted chemicals together with the DMF used during the synthesis, thus leaving behind a perfect solvent-free porous structure. This approach will be of paramount importance for a perfect understanding of the structural behavior in ZIF-7 under exposure to different gases (N_2 and CO_2). To the best of our knowledge, this study

View Article Online
DOI: 10.1039/C7TA05922A

will show for the first time that ZIF-7 is indeed able to adsorb N_2 by induction of a structural phase−to−phase transition, the total BET surface area around 380 m^2/g being rather similar to theoretical predictions.[18]

Experimental

Sample preparation

ZIF-7 nanocrystals were synthesized following the receipt described by Tu et al. [19] Briefly, 1.3784 g $Zn(NO_3)_2 \cdot 6\ H_2O$ (4.6 mmol) was dissolved in 50 ml DMF (solution A), and 1.2545 g bIm (10.6 mmol) was dissolved in 50 ml methanol (solution B). After complete dissolution, solution A was quickly poured into solution B. The mixture slowly became turbid and stirring continued up to *ca.* 30 min. The as-synthesized ZIF-7 was collected by centrifugation (7800 rpm, 1.5 h) and dried overnight at 333K (60ºC) or 403K (130ºC). Samples are labeled ZIF-7-D-60 and ZIF-7-D-130.

After the overnight drying at 333K or 403K, a portion of these samples was submitted to an additional solvent exchange process with methanol (50 ml each time) and subsequently dried at the same temperature used before (either 333K or 403K). The solvent exchange process lasted 48h. During this period the methanol solution was freshly replaced either once (samples M1) or 4 times (samples M4), to ensure the partial and complete replacement of DMF trapped in the ZIF-7 cavities by methanol. Samples are labeled ZIF-7-M1-60 and ZIF-7-M1-130 and ZIF-7-M4-60 and ZIF-7-M4-130.

View Article Online
DOI: 10.1039/C7TA05922A

Sample characterization

N_2 adsorption/desorption measurements at 77K and CO_2 adsorption measurements at 273K and 298K were performed in a home-made fully automated manometric adsorption equipment up to 1 bar. Before the adsorption measurements, samples were outgassed at 383K during 12h. Immersion calorimetry measurements were performed at 303K in a Tian-Calvet C80D calorimeter. Before the calorimetric measurement, ZIF-7 was submitted to an outgassing treatment at 383K for 12h. A full description of the experimental set-up can be found elsewhere.[20] Conventional X-ray diffraction measurements were performed using a Bruker D8-Advanced equipment with a KRISTALLOFLEX K 760-80F X-ray generator and a copper anode (λ=1.54056 Å). Scanning electron microscopy images were performed in the as-synthesized samples using a JEOL JSM-840 microscope. FTIR measurements were performed using a JASCO FTIR 4700 system in the wavenumber range from 500 to 4000 cm^{-1}, with a resolution of 4 cm^{-1}.

Synchrotron X-ray powder diffraction data (SXRPD) were collected at the high-pressure/micro-diffraction end station of the MSPD beamline at synchrotron ALBA in Spain, using a Rayonix SX165CCD 2D detector and a wavelength of 0.4243 Å.[21] The experiments were performed in *ad hoc* capillary reaction cell (fused silica capillary, inner diameter 0.7 mm, outer diameter 0.85 mm). Before the experiment the ZIF-7 samples were placed inside the capillary connected on-line to a gas-handling and vacuum line. An Oxford Cryostream 700 was used to control the temperature of the sample. *In situ* SXRPD measurements were performed at varying temperatures (80K up to 373K) and pressures (0 up to 1 bar).

View Article Online
DOI: 10.1039/C7TA05922A

Inelastic neutron scattering (INS) measurements were performed at the VISION beamline (BL-16B) of the Spallation Neutron Source (SNS), Oak Ridge National Laboratory (ORNL), USA. About 1 g of ZIF-7 was loaded in an Al sample holder connected to a gas handling system. The blank sample (ZIF-7-M4-130) was first evacuated for 1h at 298K and subsequently cooled down to 5K. Once at this temperature, the INS spectrum was collected for ≈4-6 h (the background from the instrument and sample holder is negligible in this case since the hydrogenous sample scatters neutrons very strongly). After the background measurement, ZIF-7 sample was warmed up to 77K and 1 bar of N_2 was introduced in the chamber for 1h. The dosed sample was cooled down to 5K and the INS was re-measured for ≈ 4-6 h, and compared with the spectra recorded after measuring.

Results and discussion

Samples characterization

As described above, one of the main issues when dealing with the characterization of the textural properties on a novel porous structure is the activation process, i.e. the step required before any adsorption test to ensure that all cavities have been perfectly emptied. Whereas traditionally the activation step is accomplished by a thermal treatment under vacuum for a given time, this is not always sufficient to completely remove the solvent as will be discussed later on. To avoid these drawbacks, the synthesized ZIF-7 has been submitted to several solvent exchange processes with methanol to ensure the complete removal of DMF from the inner cavities of the ZIF. To confirm the absence of DMF, the synthesized samples have

View Article Online
DOI: 10.1039/C7TA05922A

been evaluated using FTIR. At this point it is important to highlight that samples were outgassed at 383K/12h prior to the FTIR analysis. As it can be observed in Figure S1, samples without solvent exchange (ZIF-7-D-60 and ZIF-7-D-130) exhibit the characteristic peaks of DMF with the strongest band at 1670 cm^{-1} ascribed to the C=O vibrations and the methyl rocking vibration coupled with a C-N at 1090 cm^{-1}. Whereas the sample submitted to a single exchange (M1) with methanol still retains the band at 1670 cm^{-1} associated with DMF, samples submitted to a solvent exchanged 4 times (samples ZIF-7-M4-60 and ZIF-7-M4-130) does not exhibit any residual DMF, thus confirming that 4 times solvent exchange in 48h is enough to completely remove the occluded DMF.

Once the absence of DMF has been confirmed in the highly exchanged samples, the crystal structure of the synthesized materials has been evaluated using conventional X-ray diffraction (XRD) studies. Figure S2 shows the XRD pattern for the DMF-based samples and those samples exchanged 4 times with methanol (M4 samples). As it can be appreciated, all samples exhibit the characteristic pattern of the trigonal phase I (lp), commonly associated with pore occupation with guest molecules, thus suggesting that neither DMF nor methanol can be removed from the inner porosity of ZIF-7 after a drying step at 333K, or 403K in the case of DMF. Only sample ZIF-7-M4-130 exhibits a completely different XRD pattern with the characteristic background of the low symmetry distorted phase II (np). Apparently, a heat treatment at 403K overnight is not enough to remove DMF from the inner cavities of ZIF-7, in close agreement with FTIR data, while it is effective for methanol, thus leaving behind a perfectly empty cavity, in close agreement with FTIR data. In the absence of solvent, the presence of strong non-bonding interactions (van der Waals and electrostatic) in ZIF-7 favors its folding into a

View Article Online
DOI: 10.1039/C7TA05922A

high-density, highly distorted, poorly crystalline structure (phase II). Interestingly, the metal-bIm-metal bond angle changes from 49º in phase I to 29º, 54º and 63º in phase II.[14] SEM images (Figure S3) show a homogenous distribution of nano-sized particles with spherical shape, independently of the crystal structure of the material (narrow pore or large pore).

N_2 adsorption/desorption measurements at 77K

N_2 adsorption at cryogenic temperatures is the most widely applied method for the evaluation of the textural properties in nanoporous solids.[22] As described in the introduction, ZIF-7 has always being suggested in the literature as inaccessible to nitrogen at 77K.[13,18] However, theoretical calculations predict an accessible surface area of 405 m^2/g for the solvent-free ZIF-7 with a total pore volume of 0.207 cm^3/g.[18] To provide some more light in this fascinating topic, the N_2 adsorption/desorption isotherms have been evaluated at 77K (Figure 1) for the DMF-based, M1-exchanged and M4-exchanged samples. It is important to highlight that these isotherms have been evaluated under very strict criteria to reach equilibrium. For instance, under these conditions the isotherms for the M4 samples took more than 15 days to complete the adsorption and the desorption branches. Before any adsorption measurement all samples were heat treated under vacuum for 12h at 383K.

View Article Online
DOI: 10.1039/C7TA05922A

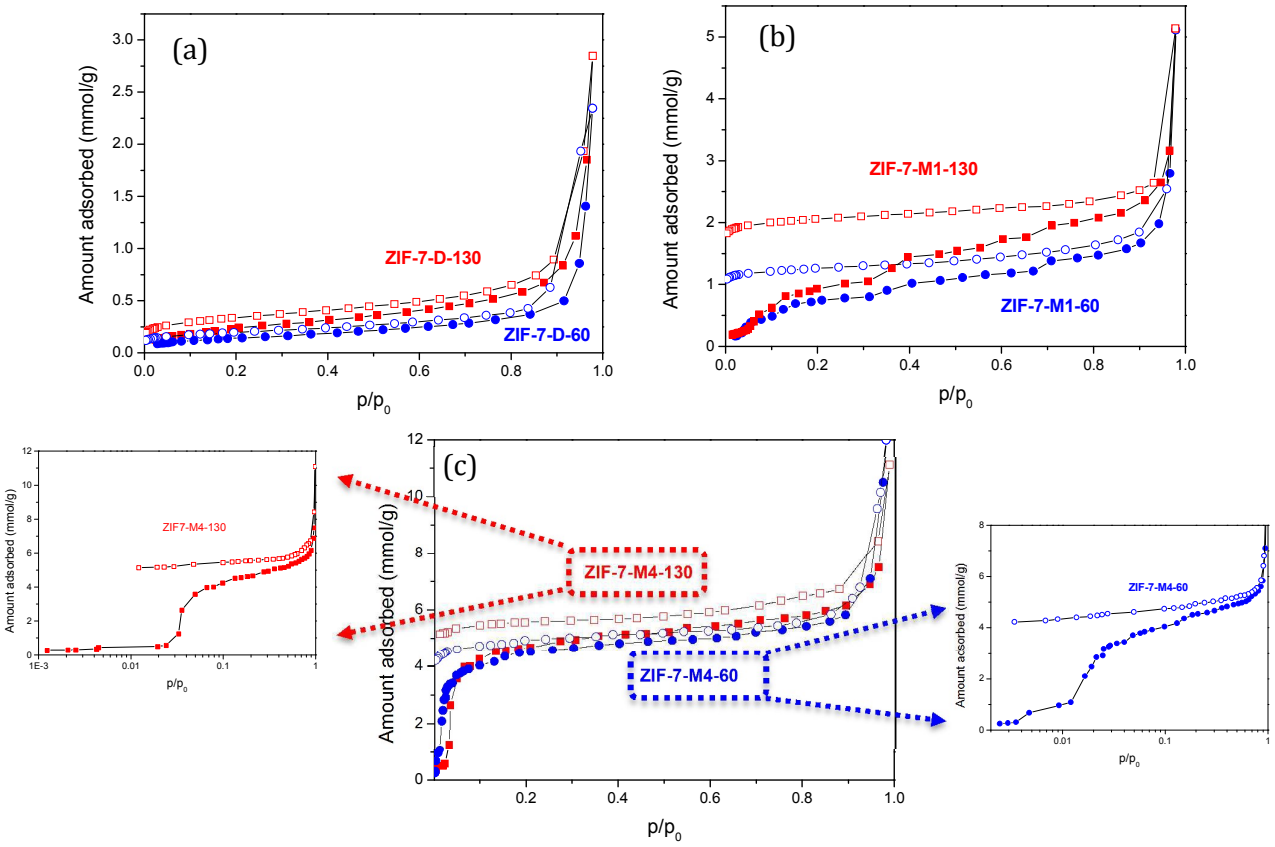

Figure 1. N_2 adsorption/desorption isotherms at 77 K for the different ZIF-7 evaluated. An amplification of the adsorption steps in samples ZIF-7-M4-60 and ZIF-7-M4-130 in logarithmic scale is also included.

Nitrogen adsorption/desorption isotherms for the DMF-based samples clearly show a complete blockage of the porosity with a relatively low adsorption capacity (< 0.7 mmol/g) up to a relative pressure of 0.8. Above this p/p_0 both samples exhibits an increase in the amount of nitrogen adsorbed due to condensation in the interparticle space. The BET surface area obtained for these samples is < 20 m^2/g, with a total pore volume of ≈ 0.01 cm^3/g. The lack of accessibility for nitrogen to the inners cavities in ZIF-7 is in close agreement with the majority of the isotherms reported in the literature so far.[13,18] The situation changes after a solvent exchange process with methanol followed by a drying step. For samples exchanged only

View Article Online
DOI: 10.1039/C7TA05922A

once with methanol (M1 samples) the nitrogen adsorption/desorption isotherms exhibit a different shape over the whole relative pressure range evaluated. Independently of the drying temperature, the isotherm exhibits a quite complex profile with multiple steps in the adsorption branch at p/p_0 around $6{\cdot}10^{-2}$, 0.12, 0.35 and 0.69, the amount adsorbed being larger in the sample dried at the higher temperature (403K). For both samples, nitrogen adsorption is irreversible with a final amount of nitrogen entrapped inside the cavities at low relative pressure (*ca.* 10^{-3} bar) of 1.07 mmol/g, for the sample dried at low temperature, and 1.82 mmol/g, for the sample treated at 403K. The BET surface area calculated for those samples is about 80-90 m^2/g and pore volume of 0.01-0.04 cm^3/g, values that are still far from the theoretical predictions by Morris et al.[18] To end up, ZIF-7 samples fully exchanged with methanol (M4 samples) were evaluated in the nitrogen adsorption process. These samples exhibit a similar adsorption profile with multiple steps at $3.5{\cdot}10^{-3}$, $1.2{\cdot}10^{-2}$, $2.4{\cdot}10^{-2}$, $4.0{\cdot}10^{-2}$, 0.13 and 0.26 (see logarithmic scale plot for clarity). Interestingly, the filling of the inner cavities for the sample dried at 403K is slightly shifted to higher relative pressures with a major step $2.5{\cdot}10^{-2}$, followed by smaller adsorption steps thereafter (see inset with logarithmic scale). Nitrogen adsorption is also irreversible with a final amount entrapped at low relative pressures (*ca.* 10^{-3} bar) of 4.29 mmol/g and 5.07 mmol/g for samples ZIF-7-M4-60 and ZIF-7-M4-130, respectively. These values give rise to a BET surface area of around 370 and 380 m^2/g, and a total pore volume of 0.17 and 0.19 cm^3/g, respectively, values that are very close to theoretical calculations.[18] At this point it is important to highlight that similar experimental studies by Morris et al. using a solvent exchange step for 3 days after the conventional DMF-based synthesis or by He et al. for ZIF-7 synthesized in the

View Article Online
DOI: 10.1039/C7TA05922A

absence of DMF (for instance using water/ethanol mixtures) reported no accessibility for N_2 up to atmospheric pressure.[13,18]

In summary, these results proof that nitrogen is indeed able to access the inner porosity in ZIF-7 when properly emptied from solvent with a final adsorption capacity that resembles theoretical predictions ($S_{BET} \approx 380$ vs. 405 m^2/g). However, these results also anticipate that N_2 can only be able to completely fill the inner cavities after an appropriate replacement of DMF with methanol (more than one exchange step is required), an appropriate activation treatment (at least 383K for 12h under vacuum) and after choosing proper equilibrium conditions (as described above, kinetics are extremely slow and more than 15 days are required to complete the isotherms). Whereas neither the drying process during the synthesis (up to 403 K) nor the outgassing treatment before the adsorption isotherms (at 383 K under vacuum) is able to remove the DMF, nitrogen adsorption measurements clearly show that this is not the case for methanol. An outgassing at 383K under high-vacuum is indeed sufficient to remove methanol and empty the inner cavities for both M4 samples.

Synchrotron X-ray powder diffraction (SXRPD) measurements

To get further knowledge about the nitrogen adsorption process in ZIF-7, sample ZIF-7-M4-130 has been evaluated using synchrotron X-ray diffraction measurements under *operando* conditions. In a first step, the sample was heat treated at 358 K for 1h under mechanical vacuum (Figure S4) before being cooled down to 80 K to get the background spectra. Afterwards the SXRPD patterns have being recorded at a constant temperature (80K) and ranging pressure from vacuum up to 1 bar N_2. Once the sample is exposed to 1 bar N_2, the capillary was

View Article Online
DOI: 10.1039/C7TA05922A

heated at increasing temperature from 80 K up to 273 K. These spectra are shown in Figure 2 and compared with the phase diagram for N_2.

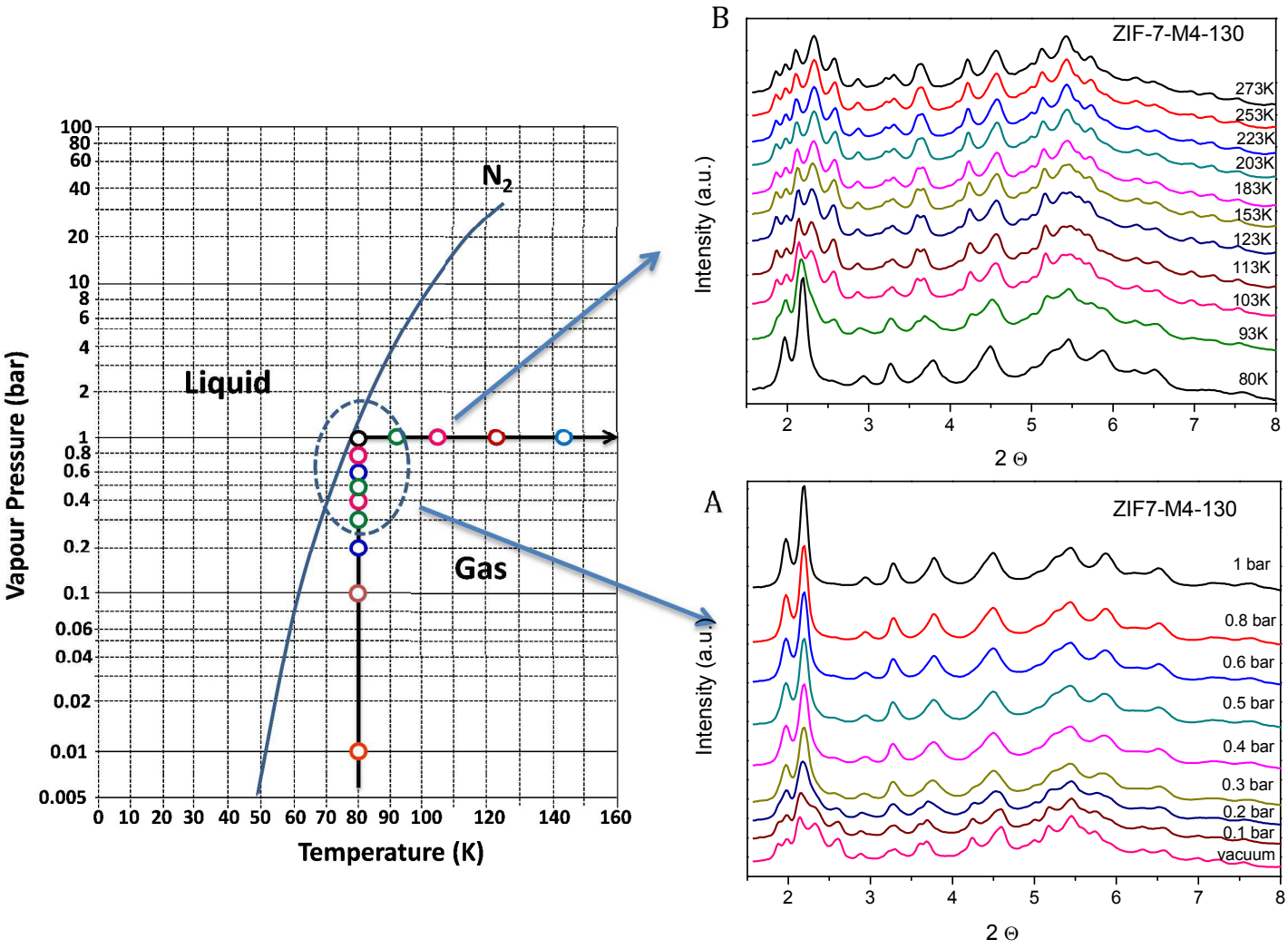

Figure 2. A. SXRPD pattern for ZIF-7-M4-130 at 80 K upon incorporation of N_2 up to 1 bar. **B.** SXRPD pattern for ZIF-7-M4-130 at 1 bar N_2 and ranging temperatures up to 273K.

As it can be observed in Figure 2A, the as-synthesized ZIF-7 at 80K exhibits the characteristic pattern of the distorted phase II, in close agreement with conventional XRD measurements described above (bottom spectra). At this point it is important to highlight that synchrotron measurements were performed several

View Article Online
DOI: 10.1039/C7TA05922A

weeks after the synthesis of the ZIF-7 sample, thus confirming that the empty phase II structure (np) is stable under normal ambient conditions for a long period. After measuring the background spectra, the capillary was dosed with increasing pressures of nitrogen up to 1 bar. As it can be appreciated in Figure 2A, upon nitrogen exposure there is a progressive change in the XRD pattern from phase II to phase I, the complete phase transition taking place at around 0.3 bar. A subsequent increase in pressure up to saturation has no effect in the XRD pattern, phase I remaining as the most stable phase for the loaded material. Once the sample reached saturation, temperature was increased from 80 K up to 273 K under 1 bar of N_2. As shown in Figure 2B, phase I remains stable up to 93K, the structure changing drastically back to phase II afterwards. Temperatures above 93K promote the desorption of the nitrogen molecules from the inner cavities of ZIF-7.

In summary, synchrotron X-ray powder diffraction data clearly evidence *for the first time* that nitrogen is indeed able to access the inner cavities in ZIF-7 via a phase transition from the guest-free phase II (np) to the gas-loaded phase I (lp) structure. Furthermore, these studies clearly show that nitrogen is stable in the inner cavities of ZIF-7 only under pressure and temperature conditions close to saturation, i.e. nitrogen requires a large driven force to induce the breathing of the ZIF-7 material.

Similar experiments were performed using sample ZIF-7-M4-60. However, as described in Figures S5-S7 only phase I (lp) was present over the whole set of experiments, i.e. it was difficult to remove methanol in the conditions used at the synchrotron (mechanical pumping instead of high vacuum and 383 K for a short period (1h)). Consequently, an activation treatment under high-vacuum for 12h, as

View Article Online
DOI: 10.1039/C7TA05922A

the one used before the N_2 adsorption measurements, seems mandatory to remove the methanol from the inner cavities in ZIF-7 pre-dried at 333 K.

Inelastic neutron scattering measurements

The vibrational and rotational pattern of ZIF-7 has been evaluated using inelastic neutron scattering measurements (INS) before and after incorporation of nitrogen on sample ZIF-7-M4-130. These experiments have been performed in the Spallation Neutron Source at Oak Ridge National Laboratory, using the VISION beamline. At the beginning of the experiment ZIF sample was evacuated for 30 min at room temperature before cooling down to 5 K to collect the background spectra. Afterwards, sample was warmed up to 77 K and 1 bar of nitrogen gas was incorporated for 1h before cooling back to 5K. To interpret the experimentally measured INS spectra, ab initio simulations of the vibrational frequencies and modes were performed using CASTEP.[23] The theoretical results were then converted to the simulated INS spectra using the aClimax software.[24] Figure 3 shows the INS before (phase II) and after (phase I) incorporation of nitrogen, in both experiment and simulation, in the energy transfer region from 0 meV up to 25 meV (upper panel) and 0 meV up to 200 meV (lower panel). As it can be appreciated, the overall agreement between experiment and simulation is excellent. Specifically, the change in the spectra upon nitrogen incorporation is qualitatively reproduced. The most significant changes can be found in the low energy range 0-25 meV, where the peak intensities are suppressed, and several sharp features are smeared out. The corresponding vibrational modes, as revealed by the ab initio calculations, are the cooperative deformation of the framework involving mainly the flapping motion of the benzimidazolate ligand with the 4- and

View Article Online
DOI: 10.1039/C7TA05922A

6-membered rings. An animation of a representative mode for narrow-pore phase II can be found in the Supplementary Information.

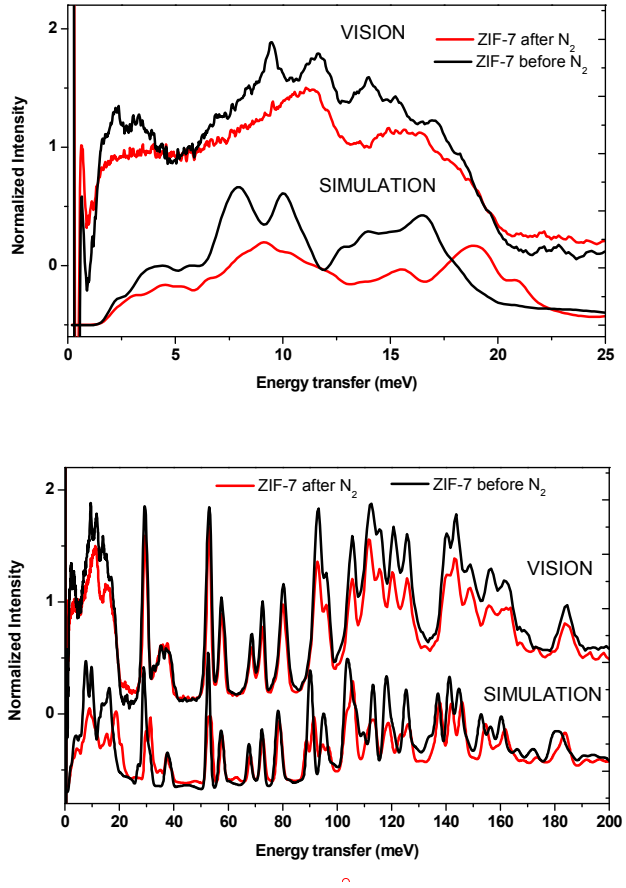

Figure 3. Inelastic neutron scattering spectra (experiment at VISION versus simulation) for ZIF-7-M4-130 sample before and after incorporation of 1 bar N_2. Upper panel shows the low energy range (0-25 meV) with the most significant changes. Lower panel shows the overall agreement between experiment and simulation in a wider energy range (0-200 meV).

This observation can be explained as below. With nitrogen filling the pores, which introduces additional electron densities along the pathways of these vibrations, it is not difficult to understand that these modes will be highly affected since they feel the presence of the nitrogen molecules most strongly. The intensities of the peaks are suppressed due to the reduced vibrational amplitude, and the peaks become much broader as the occupation of the nitrogen is likely to be disordered

View Article Online
DOI: 10.1039/C7TA05922A

and it also changes the symmetry of the host. In contrast, modes at higher frequencies (lower panel) experience much less resistance from the nitrogen, and are therefore less affected.

CO_2 adsorption measurements

To further explore the breathing phenomena under exposure to gas molecules, the synthesized ZIF-7 samples have been evaluated in the adsorption of CO_2 at 273K and 298K and up to atmospheric pressure (see Figure 4 for isotherms versus relative pressure and Figure S8 for isotherms versus total pressure). These adsorption measurements have been complemented by *in-situ* X-ray diffraction measurements performed before and after introduction of 1 bar of CO_2 (Figure S9). As it can be appreciated in Figure 4 and independently of the adsorption temperature, CO_2 is able to access the inner porosity in all synthesized samples, the amount adsorbed being rather similar for the samples partially and totally exchanged with methanol (M1 and M4 samples). These results suggest that CO_2 with a smaller kinetic diameter than nitrogen (0.33 nm vs. 0.36 nm) and at a higher adsorption temperature than nitrogen (273 K or 298 K vs. 77K) is less sensitive to the blocking effect exerted by DMF, i.e. the lower accessibility of nitrogen to the inner porosity must not a question of molecular size but rather a kinetic and/or chemical effect. Indeed, whereas the nitrogen isotherms took more than 15 days, CO_2 adsorption was rather fast (< 2 days). However, the presence of some CO_2-DMF replacement during the adsorption isotherm cannot be ruled out to explain the similar accessibility for the M1 and M4-exchanged samples.

View Article Online
DOI: 10.1039/C7TA05922A

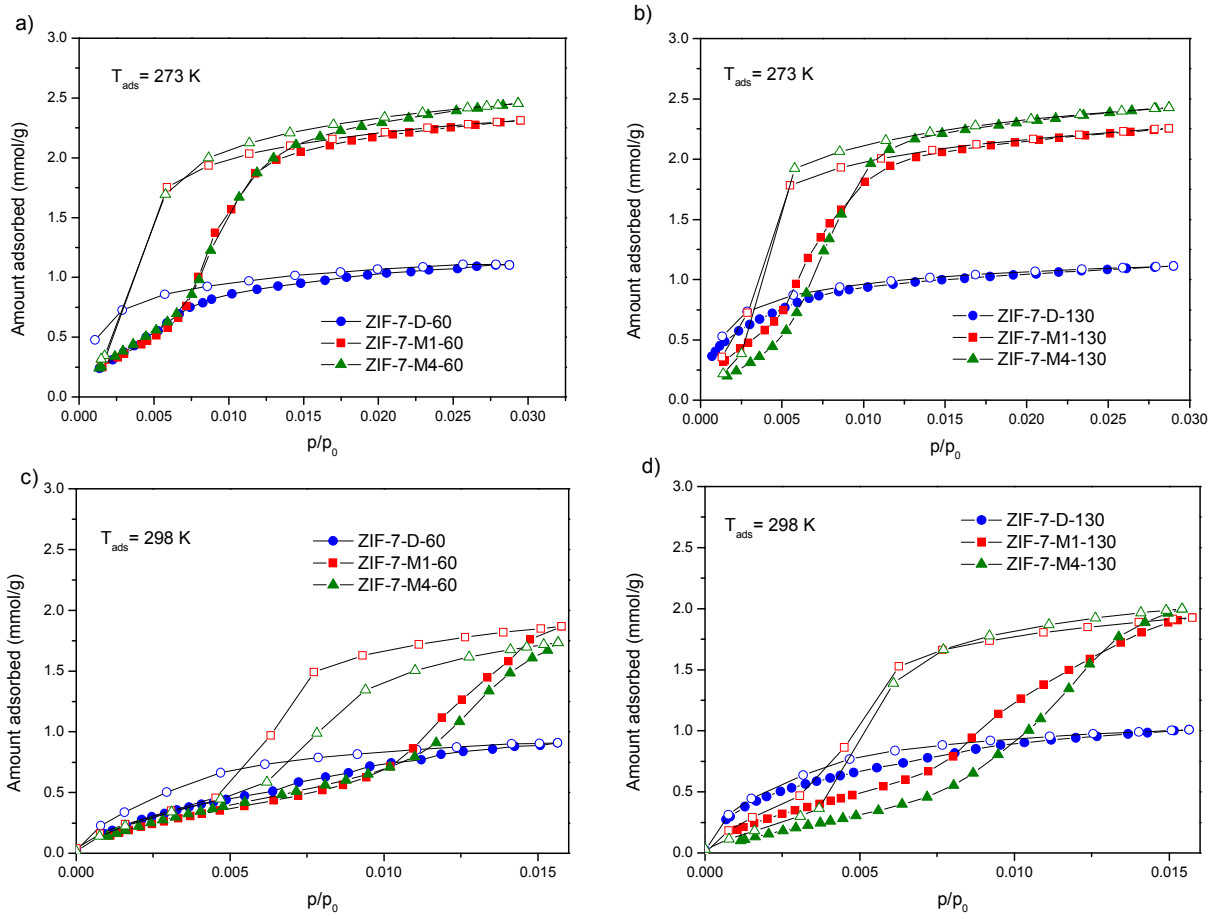

Figure 4. CO_2 adsorption/desorption isotherms at 273 K and 298 K for all ZIF-7 samples evaluated.

In general, all samples partially (M1) or totally (M4) exchanged exhibit a S-shape isotherm with a market hysteresis loop, in close agreement with previous results described in the literature.[12,16] As it can be observed in Figure S9, these adsorption isotherms are associated with a similar phase transition (phase II to phase I) as the one described above for nitrogen, i.e. incorporation of 1 bar of CO_2 at 298K gives rise to conversion from phase II (empty pore) to a phase I (guest-loaded) ZIF-7, the phase transition being fully reversible after pumping CO_2 out. The final amount adsorbed is rather similar to the values described in the literature, i.e. 2.0 mmol/g

View Article Online
DOI: 10.1039/C7TA05922A

at 273 K and 2.4 mmol/g at 298 K.[13,16,18,25] Du et al. reported a second step in the CO_2 adsorption isotherm with a final amount adsorbed up to 4.5 mmol/g, although at a lower temperature range that the one evaluated here (below 263 K).[16] Interestingly, in the specific case of CO_2 the driving force to open the ZIF-7 structure is quite independent of the adsorption temperature, the breathing of ZIF-7 taking place always at $p/p_0 \approx 0.007$-0.01. At this point it is important to highlight that compared to nitrogen, CO_2 is able to access the inner porosity in ZIF-7 at a much lower relative pressure (see for instance the phase diagram in Figure S9; CO_2 does not require to approach condensation) and with faster kinetics.

Consequently, the breathing phenomenon in ZIF-7 is not sensitive to the molecular size/shape but rather to the nature of the adsorbed molecule. The presence of specific interactions between the adsorbate and the bIm linker must be responsible for the breathing phenomena.[26,27] Apparently CO_2 can easily break down the competition between strong nonbonding interactions (van der Waals and electrostatic), which favor formation of the higher density structure, and bonding interactions (mainly torsional and bending), which are essentially harmonic and favor formation of high-symmetry, low density structures, while N_2 does not.[16] To confirm this point the XRD cell was dosed with 1 bar of nitrogen at 298 K and left for a few hours. As observed in Figure S9, ZIF-7 preserve phase II structure (empty structure) under these conditions, i.e. whereas CO_2 is able to access the inner porosity, N_2 does not.

Concerning the DMF-based ZIF-7, Figure 4 shows that all samples exhibit a type I isotherm with the low relative pressure region perfectly fitting the one of the methanol exchanged samples (except samples dried at a higher temperature). The absence of any phase transition in these samples, as suggested by XRD, clearly

View Article Online
DOI: 10.1039/C7TA05922A

suggests that the S-shape corresponds unambiguously to the breathing of the ZIF-7 structure, thus providing additional space to allocate additional CO_2 (150% more CO_2 compared to the DMF-based samples). Taking into account that the DMF-based samples are able to adsorb the same amount up to $p/p_0 \approx 0.007$-0.01, the real effect of DMF is not a blocking effect but rather an inhibition or suppression of the breathing phenomena. In the case of the sample dried at a higher temperature, the amount adsorbed in the DMF-based samples is larger at low relative pressures most probably due to the empty space left by some released DMF. In any case, the presence of residual DMF preserves ZIF-7 from breathing.

Immersion calorimetry measurements

Although theoretical calculations predicts a six-membered ring (6MR) pore entrance of ≈ 0.3 nm (cavity A) in the empty-pore ZIF-7 structure,[7] the results described above clearly show that even molecules with 0.33 nm (such as CO_2) or 0.36 nm (such as nitrogen) are able to access the inner cavities in ZIF-7, although with different kinetic. Gücüyener et al. also reported the accessibility of larger hydrocarbons, for instance C_2 and C_3 isomers to ZIF-7.[28] To get a clear experimental image of the window size in ZIF-7, sample ZIF-7-M4-130 has been evaluated using immersion calorimetry into liquids of different molecular dimensions. In the absence of specific interactions (for instance for hydrocarbons), the enthalpy of immersion can be used to estimate the accessibility of a given molecule to the inner porosity in a nanoporous solid.[20] Whereas this technique has been widely applied for activated carbons and zeolites, to our knowledge there are no reports concerning metal-organic frameworks. Figure 5 shows the evolution of the enthalpy of immersion for ZIF-7 into four different molecules, i.e.

View Article Online
DOI: 10.1039/C7TA05922A

dichloromethane (kinetic diameter 0.33 nm), n-hexane (0.43 nm), 2-methylpentane (0.5 nm) and 2,2-dimethylbutane (0.62 nm).

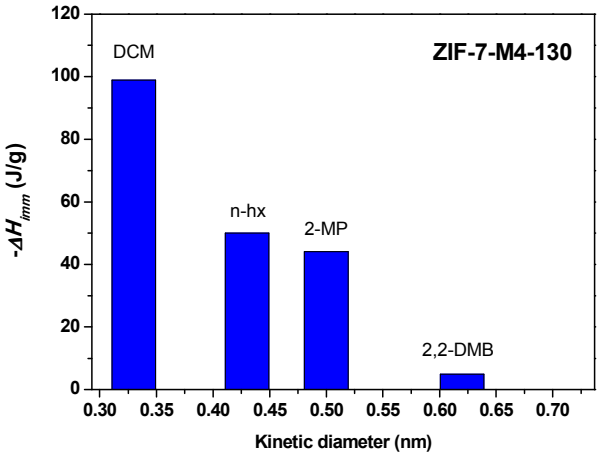

Figure 5. Enthalpy of immersion ($-\Delta H_{imm}$) of ZIF-7 into liquids of different molecular dimensions.

As it can be observed in Figure 5, the enthalpy of immersion for a small molecule such as DCM is around 100 J/g, a value very typical for a material with a highly developed and accessible porous structure. Taking into account the similar kinetic diameter for DCM (0.33 nm), CO_2 (0.33 nm) and N_2 (0.36 nm), these results confirm the above observations, i.e. all these three molecules have the proper size to access the inner cavities in ZIF-7. This result will be in close agreement with the results from Zhao et al. that predicted CO_2 to access cavity A and cavity B in ZIF-7, except the beta-cage.[29] Larger molecules such as n-hexane and 2-methylpentane gives rise to a similar enthalpy value ≈ 45-50 J/g suggesting that these two molecules are able to get into the inner porosity in ZIF-7, but not to the same extent of dichloromethane, i.e. not all cavities are accessible to n-hexane and 2-methylpentane. Interestingly, a larger molecule like 2,2-DMB (above 0.6 nm) is completely excluded, i.e. enthalpy of immersion is rather zero. Consequently,

View Article Online
DOI: 10.1039/C7TA05922A

calorimetric measurements clearly anticipate two different cavities in ZIF-7 once it opens-up, one with a window diameter below 0.4 nm (cavity A) and a second one with a pore size around 0.6 nm (cavity B), in close agreement with theoretical predictions for guest-occupied ZIF-7.[29] These results clearly anticipate the large potential of immersion calorimetry to evaluate, experimentally, the pore size window(s) in MOFs.

Conclusions

Gas adsorption studies up to atmospheric pressure clearly show that small nanocrystals of ZIF-7 are indeed able to adsorb N_2 at cryogenic temperatures, provided that the inner cavities are perfectly emptied (an extended solvent exchange with methanol is required to completely remove the DMF). Synchrotron X-ray powder analysis confirm the accessibility of nitrogen to the inner cavities in ZIF-7 associated with a breathing phenomena from a highly dense, narrow pore, phase II to a large-pore phase I. Similar experiments at room temperature and up to 1 bar anticipate that N_2 is not able to promote the breathing phenomena in ZIF-7 under these conditions, whereas CO_2, with a similar kinetic diameter does. These results confirm that the breathing in ZIF-7 highly depends on the nature of the probe adsorptive and the presence of specific interactions with the framework structure, rather than its size or shape.

ASSOCIATED CONTENT

Supporting Information. Characterization of the different MOFs synthesized (FTIR, XRD and SEM), and synchrotron and conventional X-ray powder diffraction

View Article Online
DOI: 10.1039/C7TA05922A

measurements of sample ZIF-7-M4-130 and ZIF-7-M4-60 upon gas adsorption are described in the supporting information.

AUTHOR INFORMATION

Corresponding Author

*Email: joaquin.silvestre@ua.es

ORCID

Joaquin Silvestre-Albero: 0000-0002-0303-0817

Acknowledgements

J.S.A. and C.C.C. acknowledge financial support from the University of Alicante to cover all the expenses for the INS measurements at ORNL. J.S.A. gratefully acknowledges financial support from MINECO (MAT 2013-45008-p) and Generalitat Valenciana (Prometeo2009/002), Spanish ALBA synchrotron for beam time availability (Project ID: 2016021724) and Oak Ridge beam time availability (Project ID: IPTS-16291.1). The research at the VISION beamline at ORNL´s Spallation Neutron Source was supported by the Scientific User Facilities Division, Office of Basic Energy Sciences (BES), U.S. Department of Energy (DOE), under Contract No. DE-AC0500OR22725 with UT Battelle, LLC. The computing resources were made available through the VirtuES and the ICE-MAN projects, funded by Laboratory Directed Research and Development program at ORNL.

View Article Online
DOI: 10.1039/C7TA05922A

Notes and references

1 C. Balzer, S. Braxmeier, A. Neimark, G. Reichenauer, *Langmuir* 2015, 12512-12519.
2 G.Y. Gor, O. Paris, J. Prass, P.A. Russo, M.M.L. Ribeiro Carrott, A. Neimark, *Langmuir* 2013, 29, 8601-8608.
3 P.I. Ravikovitch, A. Neimark, *Langmuir* 2006, 22, 10864-10868.
4 D. Barreda, A.M. Pérez-Mas, A. Silvestre-Albero, M.E. Casco, S. Rudic, C. Herdes, E.A. Müller, C. Blanco, R. Santamaria, J. Silvestre-Albero, F. Rodriguez-Reinoso, *Carbon* 2017, 115, 539-545.
5 K.S. Park, Z. Ni, A. Côté, J.Y. Choi, R. Huang, F.J. Uribe-Romo, H.K. Chae, M. O´Keeffe, O.M. Yaghi, *Proc. Natl. Acad. Sci.* 2006, 103, 10186-10191.
6 B. Chen, Z. Yang, Y. Zhu, Y. Xia, *J. Mater. Chem. A* 2014, 2, 16811-16831.
7 R. Banerjee, A. Phan, B. Wang, C. Knobler, H. Furukawa, M. O´Keeffe, O.M. Yaghi, *Science* 2008, 319, 939-943.
8 C.O. Ania, E. García-Pérez, M. Haro, J.J. Gutiérrez-Sevillano, T. Valdés-Solís, J.B. Parra, S. Calero, *J. Phys. Chem. Lett.* 2012, 3, 1159-1164.
9 D. Fairen-Jimenez, S.A. Moggach, M.T. Wharmby, P.A. Wright, S. Parsons, T. Düren, *J. Am. Chem. Soc.* 2011, 133, 8900-8902.
10 M.E. Casco, Y.Q. Cheng, L.L. Daemen, D. Fairen-Jimenez, E.V. Ramos-Fernandez, A.J. Ramirez-Cuesta, J. Silvestre-Albero, *Chem. Commun.* 2016, 52, 3639-3642.
11 M.E. Casco, J. Fernández-Catalá, Y.Q. Cheng, L.L. Daemen, A.J. Ramirez-Cuesta, C. Cuadrado-Collados, J. Silvestre-Albero, E.V. Ramos-Fernandez, *Chemistry Select* 2017, 2, 2750-2753.
12 S. Aguado, G. Bergeret, M. Pera Titus, V. Moizan, C. Nieto-Draghi, N. Bats, D. Farruseng, *New J. Chem.* 2011, 35, 546-550.
13 M. He, J. Yao, L. Li, K. Wang, F. Chen, H. Wang, *ChemPlusChem* 2013, 78, 1222-1225.
14 P. Zhao, G.I. Lampronti, G.O. Lloyd, M.T. Wharmby, S. Facq, A.K. Cheetham, S.A.T. Redfern, *Chem. Mater.* 2014, 26, 1767-1769.
15 W. Cai, T. Lee, M. Lee, W. Cho, D.-Y. Han, N. Choi, A.C.K. Yip, J. Choi, *J. Am. Chem. Soc.* 2014, 136, 7961-7971.
16 Y. Du, B. Wooler, M. Nines, P. Kortunov, C.S. Paur, J. Zengek, S.C. Weston, P.I. Ravikovitch, *J. Am. Chem. Soc.* 2015, 137, 13603-13611.
17 Y.-S. Li, F.-Y. Liang, H. Bux, A. Feldhoff, W.-S. Yang, J. Caro, *Angew. Chem. Int. Ed.* 2010, 49, 548-551.
18 W. Morris, N. He, K.G. Ray, P. Klonowski, H. Furukawa, I.N. Daniels, Y.A. Houndonougbo, M. Asta, O.M. Yaghi, B.B. Laird, *J. Phys. Chem. C* 2012, 116, 24084-24090.
19 M. Tu, C. Wiktor, C. Rösler, R.A. Fischer, *Chem. Commun.* 2014, 50, 13258-13260.
20 J. Silvestre-Albero, C. Gómez de Salazar, A. Sepúlveda-Escribano, F. Rodríguez-Reinoso, *Colloids and Surfaces A: Phys. & Eng. Aspects* 2001, 187-188, 151-165.
21 F. Fauth, R. Boer, F. Gil-Ortiz, C. Popescu, O. Vallcorba, I. Peral, D. Fulla, J. Benach, J. Juanhuix, *Eur. Phys. J. Plus* 2015, 130, 160-173.
22 J. Silvestre-Albero, A. Silvestre-Albero, F. Rodríguez-Reinoso, M. Thommes, *Carbon* 2012, 50, 3128-3133.
23 S.J. Clark, M.D. Segall, C.J. Pickard, P.J. Hasnip, M.J. Probert, K. Refson, M.C. Payne, *Zeitschrift für Kristallographie* 2005, 220, 567-570.

View Article Online
DOI: 10.1039/C7TA05922A

24 A.J. Ramirez-Cuesta, *Computer Physics Communications* 2004, 157, 226-238.
25 M. Pera-Titus, D. Farruseng, *J. Phys. Chem. C* 2012, 116, 1638-1649.
26 J. Seo, R. Matsuda, H. Sakamoto, C. Bonneau, S.A. Kitagawa, *J. Am. Chem. Soc.* 2009, 131, 12792-12800.
27 G. Férey, C. Serre, *Chem. Soc. Rev.* 2009, 38, 1380-1399.
28 C. Gücüyener, J. van den Bergh, J. Gascon, F. Kapteijn, *J. Am. Chem. Soc.* 2010, 132, 17704-17706.
29 P. Zhao, G.I. Lampronti, G.O. Lloyd, E. Suard, S.A.T. Redfern, *J. Mater. Chem. A* 2014, 2, 620-623.

View Article Online
DOI: 10.1039/C7TA05922A

GRAPHICAL ABSTRACT